

The Kagomé Antiferromagnet: A Schwinger-Boson Mean-Field Theory Study

Peng Li, Haibin Su

Division of Materials Science, Nanyang Technological University, 50 Nanyang Avenue, Singapore 639798

Shun-Qing Shen

Department of Physics, The University of Hong Kong, Pokfulam, Hong Kong, China

(Dated: February 9, 2022)

The Heisenberg antiferromagnet on the Kagomé lattice is studied in the framework of Schwinger-boson mean-field theory. Two solutions with different symmetries are presented. One solution gives a conventional quantum state with $\mathbf{q} = 0$ order for all spin values. Another gives a gapped spin liquid state for spin $S = 1/2$ and a mixed state with both $\mathbf{q} = 0$ and $\sqrt{3} \times \sqrt{3}$ orders for spin $S > 1/2$. We emphasize that the mixed state exhibits two sets of peaks in the static spin structure factor. And for the case of spin $S = 1/2$, the gap value we obtained is consistent with the previous numerical calculations by other means. We also discuss the thermodynamic quantities such as the specific heat and magnetic susceptibility at low temperatures and show that our result is in a good agreement with the Mermin-Wagner theorem.

PACS numbers: 75.10.Jm, 75.30.Ds, 75.40.Cx

I. INTRODUCTION

Two-dimensional (2D) geometrically frustrated Heisenberg antiferromagnets (AFMs) are potential candidates in the search of spin liquids (spin-disordered states) from both theoretical and experimental considerations. The first suggested candidate for spin liquid is the triangular lattice with nearest-neighbor (NN) couplings, but unfortunately it was finally revealed to exhibit 120° spin long-range order by extensive studies^{1,2,3,4,5}. People began to resort to interactions beyond the NN coupling to realize the spin-disordered state. Another potential candidate is the Kagomé AFM^{6,7}. It has been already known that there are two possible ordered states in this system, the so-called $\mathbf{q} = 0$ state and $\sqrt{3} \times \sqrt{3}$ state⁸ (Fig. 1), while numerical studies do not support any long range orders for the spin-1/2 system^{9,10}. This debate is still going on since numerical studies are usually limited to finite lattices. It was also investigated extensively whether the excitation spectra are gapless or not even if the system is disordered. Numerical study with up to 36 spins gives an estimation of the energy gap smaller than 1/20 of the exchange interaction¹¹. In a scenario of valence bond crystal with translational symmetry breaking, the gap of the system is found to be very small^{7,12}. Experimentally, several Kagomé-like systems have been found¹³. One of the most intriguing experimental results is the large T^2 coefficient of the specific heat of spin- $\frac{3}{2}$ $\text{SrCr}_9\text{Ga}_{12}\text{O}_{19}$ ^{14,15}, which suggests that a large linear term exists in the density of states (DOS), $D(E) \sim \eta E$. A numerical study of the spin- $\frac{1}{2}$ system suggests that the T^2 law of the specific heat can be inferred from the Heisenberg Hamiltonian with the NN couplings at very low temperatures¹⁶. A contractor renormalization calculation finds a columnar dimer order and re-produces the T^2 specific heat for the spin- $\frac{1}{2}$ system, but it still cannot tell whether it is gapless or not¹⁷. A very recent projected wavefunction study suggests that the gapless mode may be missed due to the limitation of finite lattice sites, and the gapless U(1)-Dirac state produces the T^2 specific heat¹⁸. So far many aspects of the ground state remain to be mysteries.

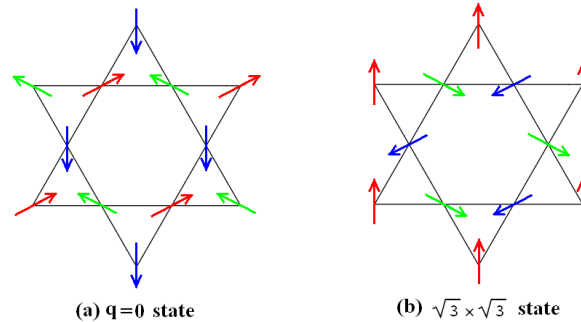


FIG. 1: (Color online) The $\mathbf{q} = 0$ and $\sqrt{3} \times \sqrt{3}$ ordered states.

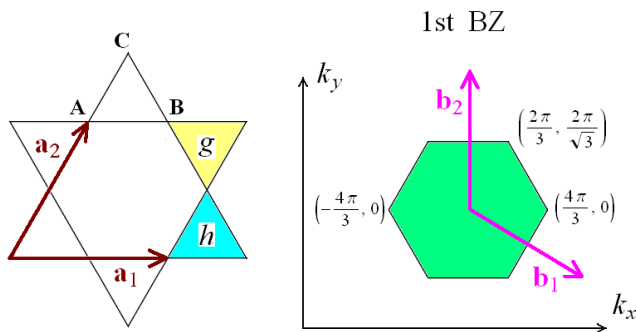


FIG. 2: (Color online) The primitive cell and the first Brillouin zone (with an area of $A_{BZ} = 8\pi^2/\sqrt{3}$) of the Kagomé lattice. The primitive translation vectors of the direct and reciprocal lattices are $(\mathbf{a}_1 = (1, 0), \mathbf{a}_2 = (1/2, \sqrt{3}/2))$ and $(\mathbf{b}_1 = (2\pi, -2\pi/\sqrt{3}), \mathbf{b}_2 = (0, 4\pi/\sqrt{3}))$, respectively.

In the theoretical aspect, it was known that the Schwinger-boson mean-field theory (SBMFT) may provide a reliable description for both quantum ordered and disordered antiferromagnets based on the picture of the resonating valence bond (RVB) state^{19,20,21}. As a merit, it does not prescribe any long-range order for the ground state in advance, which should emerge naturally if the Schwinger bosons condense at low temperatures. It was supposed that such a mean-field theory should be reliable for large spins where quantum fluctuation is believed to be weak. The theory has successfully captured the long-range order (LRO) of the Heisenberg antiferromagnets on the square^{20,21} and triangular^{22,23} lattices at zero temperature, and is in excellent agreement with the Mermin-Wagner theorem even for small spins. Of course, it also has shortcomings, such as it predicts wrongly an energy gap for a one-dimensional half-integer spin chains^{20,21}. In previous works, SBMFT had been already applied to the Kagomé system. Manuel *et. al.* gave a Schwinger-boson approach to the $\mathbf{q} = 0$ state and $\sqrt{3} \times \sqrt{3}$ state by including a third neighbour interaction²⁴. In a recent work by Wang, a new quantum disordered state is proposed for the systems with physical spin values if ring exchange interactions are introduced²⁵. In this paper, we employ SBMFT to study the Heisenberg antiferromagnet with physical spin values on the Kagomé lattice in a different approach and discover some features of the system quantities. The gauge freedom due to the geometry gives two solutions corresponding to two different types of the states⁶. The first solution gives the $\mathbf{q} = 0$ ordered state while the second solution gives a mixed state with $\mathbf{q} = 0$ order and $\sqrt{3} \times \sqrt{3}$ order for $S > \frac{1}{2}$, and a state with a very small gap for $S = \frac{1}{2}$. It was shown that the strong quantum fluctuation of quantum spin 1/2 may destroy the order states of higher spin and drive the system to be disordered. The coexistence of two orders in a quantum state is one of the key results in this paper. This result is revealed by the detailed analysis of the static spin structure factors. For the ordered states in both solutions, we show that the low-energy spectra for the quasi-particles are linear in the momentum $|\mathbf{k} - \mathbf{k}^*$ at the gapless point \mathbf{k}^* . As a result, the density of state is linear in energy, the specific heat obeys the T^2 law, and the uniform magnetic susceptibility is finite at zero temperature.

The rest of the paper is arranged as follows. The general formalism of the Schwinger-boson mean field theory is presented in Sec. II. We introduce two types of mean field parameters, and expect to capture the key features of quantum spin state on the Kagome lattice. A set of mean field equation is established by means of the Matsubara Green function techniques. In Sec. III, the numerical solutions of the mean field equations are given. We focus on the ground state properties for the system and show that the ground state of spin 1/2 has a finite energy gap to the excited states and is spin disordered while for larger spin the ground state is spin ordered. Finally, a brief discussion is presented in Sec. IV.

II. SCHWINGER-BOSON MEAN-FIELD THEORY

We start with the Heisenberg Hamiltonian on the Kagomé lattice,

$$H = J \sum_{\langle i,m;j,m' \rangle} \mathbf{S}_{i,m} \cdot \mathbf{S}_{j,m'}, \quad (1)$$

where i and j are indices of the periodic Bravais lattice, m and m' are sublattice indices, $A, B,$ or C as indicated in Fig. 2, and the notation $\langle i, m; j, m' \rangle$ means all possible NN pairs of lattice sites. The exchange interaction will be set as the unit of energy, $J = 1$. Note that the lattice constant is double of the triangle parameter l_0 and we set $2l_0 = 1$

for simplicity. We choose the primitive cell and the first Brillouin zone as in Fig. 2. In the framework of Schwinger boson theory²⁰, a pair of hard-core bosons is introduced to represent one quantum spin S at each site,

$$S_{i,m}^+ = b_{i,m,\uparrow}^\dagger b_{i,m,\downarrow}, S_{i,m}^- = b_{i,m,\downarrow}^\dagger b_{i,m,\uparrow}, S_{i,m}^z = \frac{1}{2} \left(b_{i,m,\uparrow}^\dagger b_{i,m,\uparrow} - b_{i,m,\downarrow}^\dagger b_{i,m,\downarrow} \right), \quad (2)$$

with the constraint, $b_{i,m,\uparrow}^\dagger b_{i,m,\uparrow} + b_{i,m,\downarrow}^\dagger b_{i,m,\downarrow} \equiv 2S$. In this representation, the Hamiltonian can be expressed as

$$H = - \sum_{\langle i,m;j,m' \rangle} \left(2\Delta_{i,m;j,m'}^\dagger \cdot \Delta_{i,m;j,m'} + S^2 \right) + \sum_{i,m} 2\lambda_{i,m} (b_{i,m,\uparrow}^\dagger b_{i,m,\uparrow} + b_{i,m,\downarrow}^\dagger b_{i,m,\downarrow} - 2S), \quad (3)$$

where $\Delta_{i,m;j,m'} \equiv \frac{1}{2}(b_{i,m,\uparrow} b_{j,m',\downarrow} - b_{i,m,\downarrow} b_{j,m',\uparrow})$ and N_Λ is the number of primitive cells (i.e. the total number of lattice sites is $3N_\Lambda$). The Lagrange multipliers $\lambda_{i,m}$ is introduced to realize the constraints of the number of Schwinger bosons at each site. Due to translational symmetry, we will set $\lambda_{i,m} = \lambda$ to simplify the problem. In the mean field approach, one can introduce the mean-field parameter $\langle \Delta_{i,m;j,m'} \rangle$, and decompose $\Delta_{i,m;j,m'}^\dagger \cdot \Delta_{i,m;j,m'}$ into $\langle \Delta_{i,m;j,m'}^\dagger \rangle \Delta_{i,m;j,m'} + \Delta_{i,m;j,m'}^\dagger \langle \Delta_{i,m;j,m'} \rangle - |\Delta_{i,m;j,m'}|^2$ where $\langle \dots \rangle$ represents the thermodynamic average of the physical quantity. This procedure can also be formulated equivalently as the Hubbard-Stratanovich transformation²¹. In a suitable gauge, the bond parameter $\langle \Delta_{i,m;j,m'} \rangle$ can be taken to be real²⁶. Notice there are two different solutions that can be obtained by the relation of the mean fields on the two adjacent triangles (labeled as g and h in Fig. 2). Following the spirit of Sachdev's discussion on gauge freedom of the mean-field parameter⁶, we present two schemes: (i) $\Delta = \langle \Delta_{i,m;j,m'}^g \rangle = \langle \Delta_{i,m;j,m'}^h \rangle$; (ii) $\Delta = \langle \Delta_{i,m;j,m'}^g \rangle = -\langle \Delta_{i,m;j,m'}^h \rangle$. They produce two physically distinct states that cannot be transformed into each other by gauge transformations.

In both schemes the effective Hamiltonian is decomposed into the quadratic form of $b_{i,m,\uparrow}$ and $b_{i,m,\downarrow}$, and the mean-field theories for the two schemes have almost the same formalism. In the following deduction, we shall point out their differences where it is appropriate. We can introduce three pairs of $b_{\mathbf{k},m,\mu}^\dagger$ and $b_{\mathbf{k},m,\mu}$ and $\mu = \uparrow$ or \downarrow in the Fourier transform such that the effective Hamiltonian can be written in a compact form with the help of Kronecker product,

$$H_{eff} = \sum_{\mathbf{k}} \Psi_{\mathbf{k}}^\dagger H_{mf} \Psi_{\mathbf{k}} + \varepsilon_0, \quad (4a)$$

$$H_{mf} = \lambda I_0 + \Delta \sigma_x \otimes [\gamma_1 \Omega_z - \gamma_2 \Omega_y + \gamma_3 \Omega_x] \otimes \sigma_y, \quad (4b)$$

$$\varepsilon_0 = 12N_\Lambda \Delta^2 - 6\lambda N_\Lambda (2S + 1) + 6N_\Lambda S^2, \quad (4c)$$

where the Nambu spinor is introduced

$$\Psi_{\mathbf{k}}^\dagger = (\psi_{\mathbf{k}}^\dagger, \psi_{-\mathbf{k}}), \quad \psi_{\mathbf{k}}^\dagger = (b_{\mathbf{k},A,\uparrow}^\dagger, b_{\mathbf{k},A,\downarrow}^\dagger, b_{\mathbf{k},B,\uparrow}^\dagger, b_{\mathbf{k},B,\downarrow}^\dagger, b_{\mathbf{k},C,\uparrow}^\dagger, b_{\mathbf{k},C,\downarrow}^\dagger), \quad (5)$$

I_0 is a 12×12 unit matrix, σ_α ($\alpha = x, y, z$) are 2×2 Pauli matrices, Ω_α ($\alpha = x, y, z$) are 3×3 Hermitian matrices

$$\Omega_x = \begin{pmatrix} 0 & 0 & 0 \\ 0 & 0 & -i \\ 0 & i & 0 \end{pmatrix}, \Omega_y = \begin{pmatrix} 0 & 0 & i \\ 0 & 0 & 0 \\ -i & 0 & 0 \end{pmatrix}, \Omega_z = \begin{pmatrix} 0 & -i & 0 \\ i & 0 & 0 \\ 0 & 0 & 0 \end{pmatrix}, \quad (6)$$

and for the two schemes we have (i) $\gamma_1 = \cos \frac{k_x}{2}$, $\gamma_2 = \cos \frac{k_x + \sqrt{3}k_y}{4}$, $\gamma_3 = \cos \frac{k_x - \sqrt{3}k_y}{4}$; and (ii) $\gamma_1 = \sin \frac{k_x}{2}$, $\gamma_2 = \sin \frac{k_x + \sqrt{3}k_y}{4}$, $\gamma_3 = \sin \frac{k_x - \sqrt{3}k_y}{4}$, respectively.

Let us define the Matsubara Green's function (a 12×12 matrix) by the outer product of the Nambu spinor Eq. (5),

$$G(\mathbf{k}, \tau) = - \left\langle T_\tau \Psi_{\mathbf{k}}(\tau) \Psi_{\mathbf{k}}^\dagger \right\rangle, \quad (7)$$

where τ is the imaginary time and $\Psi_{\mathbf{k}}(\tau) = e^{\tau H_{eff}} \Psi_{\mathbf{k}} e^{-\tau H_{eff}}$. Then physical quantities concerning the average of two operators can be readily expressed by the matrix elements, e.g. $\langle b_{\mathbf{k},1,\uparrow} b_{\mathbf{k},1,\uparrow}^\dagger \rangle = -G_{1,1}(\mathbf{k}, \tau = 0^+)$. And the physical quantities concerning the average of four operators, such as the correlation functions, can be decomposed into the averages of two operators through the Wick theorem. We shall use these facts to establish the mean-field equations and the static spin structure factors later.

It is easy to prove that the Matsubara Green's function in Matsubara frequency $\omega_n = 2n\pi/\beta$ (n is an integer for bosons) can be worked out by (also a 12×12 matrix)

$$G(\mathbf{k}, i\omega_n) = [i\omega_n \sigma_z \otimes \Omega_0 \otimes \sigma_0 - H_{mf}]^{-1}, \quad (8)$$

where Ω_0 and σ_0 are 3×3 and 2×2 unit matrices. Because of symmetry, some elements are the same. Fortunately, these functions can be calculated analytically, and the lengthy expressions will be presented elsewhere. From the poles of single particle Matsubara function, the six branches of the energy spectra of quasi-particles can be read out in the first Brillouin zone. Two are the flat bands $\omega_{1,\mu} = \lambda$ and other four-fold degenerate bands are $\omega_{2,\mu}(\mathbf{k}) = \omega_{3,\mu}(\mathbf{k}) = \omega(\mathbf{k})$ with $\omega(\mathbf{k}) = \sqrt{\lambda^2 - \Delta^2 \gamma^2(\mathbf{k})}$ with $\gamma^2(\mathbf{k}) = \gamma_1^2 + \gamma_2^2 + \gamma_3^2$. The mean-field parameter Δ and the Lagrangian multiplier λ should be determined self-consistently. The mean field can be evaluated by reading the elements of the Matsubara Green function matrix after the Fourier transformation, e.g.

$$\begin{aligned} \Delta &= \frac{1}{2} (\langle b_{i,A,\uparrow} b_{i,B,\downarrow} \rangle - \langle b_{i,A,\downarrow} b_{i,B,\uparrow} \rangle) \\ &= \frac{-1}{2\beta N_\Lambda} \sum_{\mathbf{k}, i\omega_n} e^{-ik_x/2 - i\omega_n 0^+} [G_{10,1}(\mathbf{k}, i\omega_n) + G_{9,2}(\mathbf{k}, i\omega_n)]. \end{aligned} \quad (9)$$

Another constraint is that we should use the average value in the thermodynamic limit $\langle b_{i,m,\uparrow}^\dagger b_{i,m,\uparrow} + b_{i,m,\downarrow}^\dagger b_{i,m,\downarrow} \rangle = 2S$ to replace the original constraint. These two facts lead to a set of the mean-field equations for Δ and λ ,

$$3S + 1 = 2n_B(\lambda) + \frac{1}{N_\Lambda} \sum_{\mathbf{k}} \frac{\lambda}{\omega(\mathbf{k})} [1 + 2n_B(\omega(\mathbf{k}))], \quad (10a)$$

$$\Delta = \frac{1}{6} \frac{1}{N_\Lambda} \sum_{\mathbf{k}} \frac{\Delta \gamma^2(\mathbf{k})}{\omega(\mathbf{k})} [1 + 2n_B(\omega(\mathbf{k}))], \quad (10b)$$

where $n_B(\omega(\mathbf{k})) = [e^{\omega(\mathbf{k})/T} - 1]^{-1}$ is the Bose-Einstein distribution function with temperature T . In the thermodynamical limit $N_\Lambda \rightarrow \infty$, the momentum sum is replaced by the integral over the first Brillouin zone (Fig. 2), $\frac{1}{N_\Lambda} \sum_{\mathbf{k}} \rightarrow \int \frac{d^2k}{A_{BZ}}$, where $A_{BZ} = \frac{8\pi^2}{\sqrt{3}}$ is the area of the first Brillouin zone. When the Schwinger bosons condensation occurs, i.e. the solution gives a gapless spectrum $\omega(\mathbf{k}^*) = 0$, we can extract a condensation term²¹ in the momentum summation of the first equation, Eq. (10a),

$$\rho_0(T) = \frac{\lambda}{N_\Lambda \omega(\mathbf{k}^*)} [1 + 2n_B(\omega(\mathbf{k}^*))]. \quad (11)$$

With the help of the mean-field equations at zero temperature, we can obtain the simplified form of ground energy per bond

$$E_0/6N_\Lambda = -2\Delta^2 + S^2. \quad (12)$$

III. SOLUTIONS

To solve the mean-field equations, let us introduce dimensionless quantities, $\tilde{\Delta} = \frac{\Delta}{\lambda}$ and $\tilde{T} = \frac{T}{\lambda}$. Then the mean-field equations become,

$$3S + 1 = \coth\left(\frac{1}{2\tilde{T}}\right) - 1 + \rho_0(\tilde{T}) + I_0(\tilde{T}), \quad (13a)$$

$$\Delta = \frac{\tilde{\Delta} \gamma^2(\mathbf{k}^*)}{6} \rho_0(\tilde{T}) + I_1(\tilde{T}), \quad (13b)$$

with the definitions of two integrals

$$I_0(\tilde{T}) = \int \frac{d^2k}{A_{BZ}} \frac{1}{\sqrt{1 - \tilde{\Delta}^2 \gamma^2(\mathbf{k})}} \coth \frac{\sqrt{1 - \tilde{\Delta}^2 \gamma^2(\mathbf{k})}}{2\tilde{T}}, \quad (14a)$$

$$I_1(\tilde{T}) = \frac{1}{6} \int \frac{d^2k}{A_{BZ}} \frac{\tilde{\Delta} \gamma^2(\mathbf{k})}{\sqrt{1 - \tilde{\Delta}^2 \gamma^2(\mathbf{k})}} \coth \frac{\sqrt{1 - \tilde{\Delta}^2 \gamma^2(\mathbf{k})}}{2\tilde{T}}. \quad (14b)$$

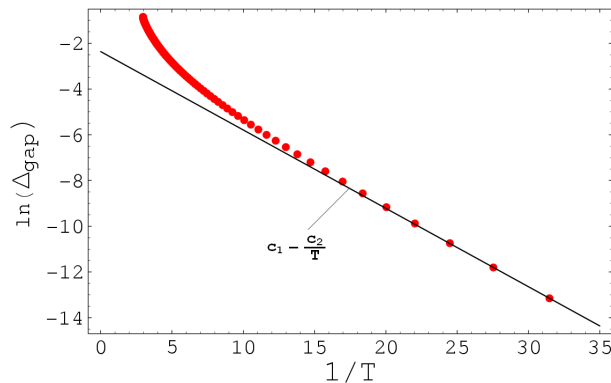


FIG. 3: (Color online) The asymptotic behavior of the gap near zero temperature for the case of $S = 1/2$ in scheme (i). The dots are numerical solutions. The solid line is a linear fit with $c_1 \approx -2.36$ and $c_2 \approx 0.34$, which gives $\Delta_{gap} \approx 0.094e^{-0.34/T}$ as $T \rightarrow 0$.

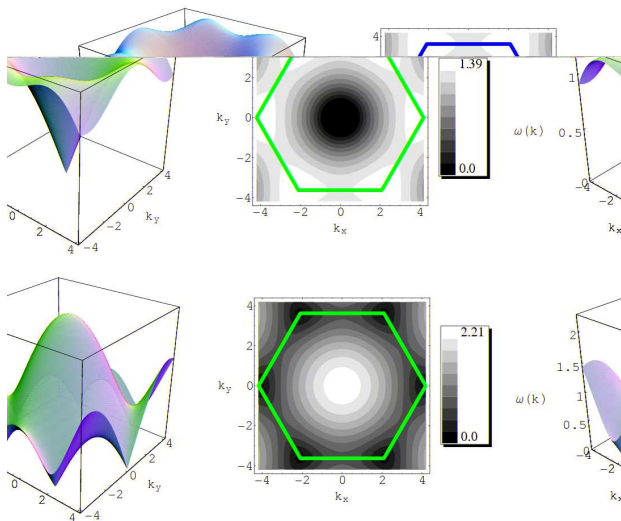


FIG. 4: (Color online) The cone-shaped quasiparticle spectra for the gapless solutions. Here we set $S = 3/2$. The upper spectrum is for scheme (i). The lower one is for scheme (ii). The interior area of the blue hexagon is the first Brillouin zone.

First, we solve the equations at zero temperature. For the scheme (i), we found the first integral is bounded from above by the value $I_0 = 1.75097$ at $\tilde{\Delta} = \frac{1}{\sqrt{3}}$. We notice that a nonzero condensation density persists as long as $S \geq S_c \approx 0.25032$. Numerical solutions are $\rho_0 = 3S - 0.75097$, $\Delta = \frac{\sqrt{3}}{2}S + 0.091132$, and $\lambda = \frac{3}{2}S + 0.15785$. The condensation occurs at the Γ point, $\mathbf{k}^* = (0, 0)$. For the scheme (ii) we find that the first integral is bounded from above by the value $I_0 = 2.68932$ at $\tilde{\Delta} = \frac{2}{3}$ and the critical spin value is $S_c \approx 0.5631$. Thus for $S = \frac{1}{2}$, we obtain a spin liquid because the spectrum is gapped with numerical solution $\rho_0 = 0$, $\Delta = 0.493757$, and $\lambda = 0.741905$. The value of the gap is $\Delta_{gap} = 0.0434$, which is coincident with the recent numerical estimation that the gap is smaller than $\frac{1}{20}^{11}$. For larger spins $S > \frac{1}{2}$, numerical solutions are $\rho_0 = 3S - 1.68932$, $\Delta = \frac{3}{4}S + 0.118784$, and $\lambda = \frac{9}{8}S + 0.178176$. The condensation occurs at six corner K points, e.g. $\mathbf{k}^* = (\frac{4\pi}{3}, 0)$.

Now, we discuss the asymptotic behavior of the solution near zero temperature. Our numerical results show that the condensation only occurs at zero temperature, which is in agreement with the Mermin-Wagner theorem for two-dimensional Heisenberg systems. Numerical calculations tell us that the gapless solution can only exist at zero temperature and an energy gap opens at finite temperature, which behaves as $\Delta_{gap} \propto e^{-c/T}$ as $T \rightarrow 0$. We give an example for the case of $S = \frac{1}{2}$ in the scheme (i). The curve for $\ln \Delta_{gap} \sim \frac{1}{T}$ is plotted in Fig. 3. The lowest finite temperature we approach is $T \approx 0.03177$ (in unit of coupling J), where we get a small gap $\Delta_{gap} \approx 1.944 \times 10^{-6}$.

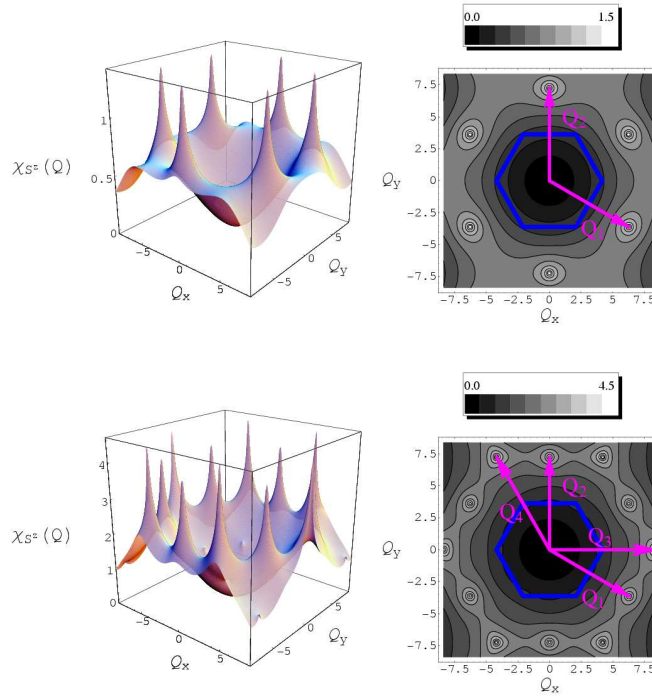


FIG. 5: (Color online) The spin structure factors $\chi_{S^z}(\mathbf{Q})$ for the two mean-field schemes in the text. The upper one is for scheme (i), and the lower one is for scheme (ii). Here we set $S = 3/2$. The divergent peaks signal the existence of LRO. Other spin values have similar results, except for the case of $S = 1/2$ in scheme (ii), where the peaks are of finite height because the solution is gapped. The interior area of the blue hexagon is the first Brillouin zone.

In the following, we turn to the relevant thermodynamical quantities and the patterns of LRO at zero temperature. The gapless spectra for both ordered states are exemplified in Fig. 4. It is clear that the cone-shaped spectra are linear in the momentum

$$\omega(\mathbf{k}) \approx \alpha |\mathbf{k} - \mathbf{k}^*|, \quad (15)$$

where $\alpha = \frac{\lambda}{2\sqrt{2}}$ for the scheme (i) and $\alpha = \frac{\lambda}{2\sqrt{3}}$ for the scheme (ii). Correspondingly, the density of state (DOS) of the quasiparticles linear in the low energy,

$$D(E) \approx \eta E + O(E^3), \quad (16)$$

where $\eta = \frac{8\sqrt{3}}{\pi\lambda^2}$ for the scheme (i) and $\eta = \frac{24}{\pi\lambda^2}$ for the scheme (ii). As a result, the T^2 law of specific heat is anticipated for both ordered states

$$C_V/N_\Lambda \sim 6\zeta(3)\eta \left(\frac{T}{J}\right)^2 \quad (17)$$

at very low temperatures.

The non-zero value of ρ_0 means the condensation of the quasi-particles and the existence of LRO at zero-temperature. To disclose the ordered patterns of the ground states we need to calculate the static spin structure factor

$$\chi_{S^z}(\mathbf{Q}) = \lim_{\tau \rightarrow 0} \langle T_\tau S_{\mathbf{Q}}^z(\tau) S_{-\mathbf{Q}}^z \rangle, \quad (18)$$

where τ is the imaginary time and $S_{\mathbf{Q}}^z = \frac{1}{\sqrt{N_\Lambda}} \sum_{i,m} S_{i,m}^z e^{i\mathbf{Q}\cdot\mathbf{r}_{i,m}}$. A detailed calculation shows that the static spin structure factor is isotropic, $\langle S_{\mathbf{Q}}^x S_{-\mathbf{Q}}^x \rangle = \langle S_{\mathbf{Q}}^y S_{-\mathbf{Q}}^y \rangle = \langle S_{\mathbf{Q}}^z S_{-\mathbf{Q}}^z \rangle$, which indicates that the ground state is invariant under the spin rotation. Analytically, we have that the total spin $\langle \mathbf{S}_{tot}^2 \rangle = 3N_\Lambda \chi_{S^z}(0) = 0$ for both ordered states, which is consistent with the consequence of exact diagonalization techniques for^{9,11}. The divergent peaks of $\chi_{S^z}(\mathbf{Q})$ signal the existence of LRO as shown in Fig. 5. (Notice that for the case of $S = 1/2$ in the scheme (ii), the peaks are

of finite height because the solution is gapped. We do not show it here.) Careful calculation shows the value of the divergent peak is proportional to the number of primitive cells

$$\chi_{S^z}(\mathbf{Q}^*) \propto \frac{\lambda^2 [1 + 2n_B(\omega(\mathbf{k}^*))][1 + 2n_B(\omega(\mathbf{k}^* + \mathbf{Q}^*))]}{N_\Lambda \omega(\mathbf{k}^*) \omega(\mathbf{k}^* + \mathbf{Q}^*)} = N_\Lambda \rho_0^2. \quad (19)$$

\propto Notice the primitive cell contains more than one site, the replicative area of $\chi_{S^z}(\mathbf{Q})$ is 4 times of the area of the first Brillouin zone A_{BZ} (Fig. 5). This can be easily verified by the definition, Eq. (18).

For the scheme (i), a characteristic feature of the static structure factor $\chi_{S^z}(\mathbf{Q})$ is the six divergent peaks, which are located at the wave vectors, $\mathbf{Q}^* \in \{\pm\mathbf{Q}_1, \pm\mathbf{Q}_2, \pm(\mathbf{Q}_1 + \mathbf{Q}_2)\}$ with $\mathbf{Q}_1 = \mathbf{b}_1$ and $\mathbf{Q}_2 = \mathbf{b}_2$. At the divergent peaks, say e.g. at $\mathbf{Q} = \pm\mathbf{Q}_1$, one gets $S_{\pm\mathbf{Q}_1}^z = \frac{1}{\sqrt{N_\Lambda}} \sum_i (S_{i,A}^z + e^{\pm i\pi} S_{i,B}^z + S_{i,C}^z)$. Combining it with the facts that, $\chi_{S^z}(0) = 0$, we draw a conclusion that the configuration of LRO has the $\mathbf{q} = 0$ order. The $\mathbf{q} = 0$ order is marked by the neutron scattering peak at the distance

$$|\mathbf{Q}_1| = \frac{4\pi}{\sqrt{3}}. \quad (20)$$

should mark the neutron scattering peak position.

For the scheme (ii), a similar analysis leads to another type of order pattern. In this case the divergent peaks are located at the wave vectors, $\mathbf{Q}^* \in \{\pm\mathbf{Q}_1, \pm\mathbf{Q}_2, \pm(\mathbf{Q}_1 + \mathbf{Q}_2), \pm\mathbf{Q}_3, \pm\mathbf{Q}_4, \pm(\mathbf{Q}_3 + \mathbf{Q}_4)\}$ with $\mathbf{Q}_3 = \frac{2}{3}(2\mathbf{b}_1 + \mathbf{b}_2)$ and $\mathbf{Q}_4 = \frac{2}{3}(-\mathbf{b}_1 + \mathbf{b}_2)$. The patterns corresponding \mathbf{Q}_3 and \mathbf{Q}_4 peaks are the usual $\sqrt{3} \times \sqrt{3}$ order (Fig. 1). So for the scheme (ii) we obtain a solution with mixed $\mathbf{q} = 0$ order and $\sqrt{3} \times \sqrt{3}$ order. Notice the mixture of two orders originate from quantum mechanical superposition. This may be an exotic state with coexistence of two distinct orders. The $\sqrt{3} \times \sqrt{3}$ order is marked by neutron scattering peak at the distance

$$|\mathbf{Q}_3| = \frac{8\pi}{3}. \quad (21)$$

Our calculation found the peak at $|\mathbf{Q}_3|$ is a little stronger than that at $|\mathbf{Q}_1|$, since the ratio of the two sets of divergent peaks is

$$\frac{\chi_{S^z}(\mathbf{Q}_3)}{\chi_{S^z}(\mathbf{Q}_1)} = \frac{3}{2}. \quad (22)$$

The uniform magnetic susceptibility can be obtained by the analytic continuation

$$\begin{aligned} \chi_M &= \lim_{\mathbf{Q} \rightarrow 0} \lim_{i\omega_n \rightarrow 0} \chi_{S^z}(\mathbf{Q}, i\omega_n) \\ &= \int \frac{d^2k}{A_{BZ}} \frac{\Delta^4 [\gamma_1^2 \gamma_2^2 + \gamma_2^2 \gamma_3^2 + \gamma_3^2 \gamma_1^2]}{2\omega(\mathbf{k}) [\lambda - \omega(\mathbf{k})] [\lambda + \omega(\mathbf{k})]^3}. \end{aligned} \quad (23)$$

χ_M has a finite value at zero temperature since the divergent denominator is annihilated by the linear DOS, $\chi_M \sim \int D(E) \frac{1}{E} dE \sim \text{finite}$.

IV. DISCUSSION

There are several materials which possess the structures of the spin Kagomé lattice. Experimental data by Muon Spin Relaxation show that the compound $\text{SrCr}_{8-x}\text{Ga}_{4+x}\text{O}_{19}$ lacks a long-range order until 0.05K^{27} . The entropy measurement of the same compound gives a T^2 law for the specific heat at low temperatures, which was regarded as an evidence to support the absence of long-range order¹⁵. However, spontaneous breaking of a continuous symmetry produces massless Goldstone modes²⁸, and LRO can only exist at zero temperature for 2D systems according to Mermin-Wagner theorem²¹. From the present calculation of SBMFT, the special structure of the Kagomé lattice leads to the cone structure of the spectra for the quasi-particles in the momentum space. The existence of long-range correlation is consistent with the picture of the gapless spectrum of quasi-particles and the ordered ground state can produce the T^2 law of the specific heat. Of course, the possible existence of the additional next-nearest-neighbor coupling could further weaken the long-range correlation.

We thank C. Broholm for helpful discussions. This work was supported by the COE-SUG Grant (No. M58070001) of NTU and the Research Grant Council of Hong Kong under Grant No.: HKU 703804.

APPENDIX A: STATIC SPIN STRUCTURE FACTORS

The spin structure factor at zero temperature (see Fig. 5) contains both intra-sublattice and inter-sublattice contributions,

$$\begin{aligned}
\chi_S(\mathbf{Q}) &= \langle S_{\mathbf{Q}}^z S_{-\mathbf{Q}}^z \rangle = \frac{1}{N_{\Lambda}} \sum_{m,n \in A,B,C} \langle S_m^z S_n^z \rangle e^{i\mathbf{Q} \cdot (\mathbf{r}_m - \mathbf{r}_n)} \\
&= \chi_{AA}(\mathbf{Q}) + \chi_{BB}(\mathbf{Q}) + \chi_{CC}(\mathbf{Q}) \\
&\quad + \chi_{AB}(\mathbf{Q}) + \chi_{BA}(\mathbf{Q}) + \chi_{AC}(\mathbf{Q}) \\
&\quad + \chi_{CA}(\mathbf{Q}) + \chi_{BC}(\mathbf{Q}) + \chi_{CB}(\mathbf{Q})
\end{aligned} \tag{A1}$$

where we have defined the spin density wave operator

$$S_{\mathbf{Q}}^z = \sum_{m \in A,B,C} S_m^z e^{i\mathbf{Q} \cdot \mathbf{r}_m}. \tag{A2}$$

The intra-sublattice and inter-sublattice contributions are

$$\chi_{AA}(\mathbf{Q}) = \int \frac{d^2k}{2A_{BZ}} [O_{a12}(\mathbf{k} + \mathbf{Q}) + P_{a12}(\mathbf{k} + \mathbf{Q})] Q_{a12}(\mathbf{k}),$$

$$\chi_{BB}(\mathbf{Q}) = \int \frac{d^2k}{2A_{BZ}} [O_{a2}(\mathbf{k} + \mathbf{Q}) + P_{a13}(\mathbf{k} + \mathbf{Q})] Q_{a13}(\mathbf{k}),$$

$$\chi_{CC}(\mathbf{Q}) = \int \frac{d^2k}{2A_{BZ}} [O_{a1}(\mathbf{k} + \mathbf{Q}) + P_{a23}(\mathbf{k} + \mathbf{Q})] Q_{a23}(\mathbf{k}),$$

$$\begin{aligned}
\chi_{AB}(\mathbf{Q}) &= \chi_{BA}(\mathbf{Q}) \\
&= \int \frac{d^2k}{2A_{BZ}} \{ [-O_{b23}(\mathbf{k} + \mathbf{Q}) + P_{b23}(\mathbf{k} + \mathbf{Q})] Q_{b23}(\mathbf{k}) - R_1(\mathbf{k}) R_1(\mathbf{k} + \mathbf{Q}) \},
\end{aligned}$$

$$\begin{aligned}
\chi_{BC}(\mathbf{Q}) &= \chi_{CB}(\mathbf{Q}) \\
&= \int \frac{d^2k}{2A_{BZ}} \{ [-O_{b13}(\mathbf{k} + \mathbf{Q}) + P_{b13}(\mathbf{k} + \mathbf{Q})] Q_{b13}(\mathbf{k}) - R_2(\mathbf{k}) R_2(\mathbf{k} + \mathbf{Q}) \},
\end{aligned}$$

$$\begin{aligned}
\chi_{CA}(\mathbf{Q}) &= \chi_{AC}(\mathbf{Q}) \\
&= \int \frac{d^2k}{2A_{BZ}} \{ [-O_{b12}(\mathbf{k} + \mathbf{Q}) + P_{b12}(\mathbf{k} + \mathbf{Q})] Q_{b12}(\mathbf{k}) - R_3(\mathbf{k}) R_3(\mathbf{k} + \mathbf{Q}) \},
\end{aligned}$$

where

$$O_{a1}(\mathbf{k}) = \frac{\Delta^2 \gamma_1^2(\mathbf{k})}{1 - \omega^2(\mathbf{k})}, O_{a2}(\mathbf{k}) = \frac{\Delta^2 \gamma_2^2(\mathbf{k})}{1 - \omega^2(\mathbf{k})}, O_{a3}(\mathbf{k}) = \frac{\Delta^2 \gamma_3^2(\mathbf{k})}{1 - \omega^2(\mathbf{k})},$$

$$P_{a12}(\mathbf{k}) = \frac{\Delta^2 [\gamma_1^2(\mathbf{k}) + \gamma_2^2(\mathbf{k})]}{2\omega(\mathbf{k}) [1 - \omega(\mathbf{k})]}, P_{a13}(\mathbf{k}) = \frac{\Delta^2 [\gamma_1^2(\mathbf{k}) + \gamma_3^2(\mathbf{k})]}{2\omega(\mathbf{k}) [1 - \omega(\mathbf{k})]}, P_{a23}(\mathbf{k}) = \frac{\Delta^2 [\gamma_3^2(\mathbf{k}) + \gamma_2^2(\mathbf{k})]}{2\omega(\mathbf{k}) [1 - \omega(\mathbf{k})]},$$

$$Q_{a12}(\mathbf{k}) = \frac{\Delta^2 [\gamma_1^2(\mathbf{k}) + \gamma_2^2(\mathbf{k})]}{2\omega(\mathbf{k}) [1 + \omega(\mathbf{k})]}, Q_{a13}(\mathbf{k}) = \frac{\Delta^2 [\gamma_1^2(\mathbf{k}) + \gamma_3^2(\mathbf{k})]}{2\omega(\mathbf{k}) [1 + \omega(\mathbf{k})]}, Q_{a23}(\mathbf{k}) = \frac{\Delta^2 [\gamma_3^2(\mathbf{k}) + \gamma_2^2(\mathbf{k})]}{2\omega(\mathbf{k}) [1 + \omega(\mathbf{k})]},$$

$$O_{b23}(\mathbf{k}) = \frac{\Delta^2 \gamma_3(\mathbf{k}) \gamma_2(\mathbf{k})}{1 - \omega^2(\mathbf{k})}, O_{b13}(\mathbf{k}) = \frac{\Delta^2 \gamma_1(\mathbf{k}) \gamma_3(\mathbf{k})}{1 - \omega^2(\mathbf{k})}, O_{b12}(\mathbf{k}) = \frac{\Delta^2 \gamma_1(\mathbf{k}) \gamma_2(\mathbf{k})}{1 - \omega^2(\mathbf{k})},$$

$$P_{b23}(\mathbf{k}) = \frac{\Delta^2 \gamma_3(\mathbf{k}) \gamma_2(\mathbf{k})}{2\omega(\mathbf{k}) [1 - \omega(\mathbf{k})]}, P_{b13}(\mathbf{k}) = \frac{\Delta^2 \gamma_1(\mathbf{k}) \gamma_3(\mathbf{k})}{2\omega(\mathbf{k}) [1 - \omega(\mathbf{k})]}, P_{b12}(\mathbf{k}) = \frac{\Delta^2 \gamma_1(\mathbf{k}) \gamma_2(\mathbf{k})}{2\omega(\mathbf{k}) [1 - \omega(\mathbf{k})]},$$

$$Q_{b23}(\mathbf{k}) = \frac{\Delta^2 \gamma_3(\mathbf{k}) \gamma_2(\mathbf{k})}{2\omega(\mathbf{k}) [1 + \omega(\mathbf{k})]}, Q_{b13}(\mathbf{k}) = \frac{\Delta^2 \gamma_1(\mathbf{k}) \gamma_3(\mathbf{k})}{2\omega(\mathbf{k}) [1 + \omega(\mathbf{k})]}, Q_{b12}(\mathbf{k}) = \frac{\Delta^2 \gamma_1(\mathbf{k}) \gamma_2(\mathbf{k})}{2\omega(\mathbf{k}) [1 + \omega(\mathbf{k})]},$$

$$R_1(\mathbf{k}) = \frac{\Delta \gamma_1(\mathbf{k})}{2\omega(\mathbf{k})}, R_2(\mathbf{k}) = \frac{\Delta \gamma_2(\mathbf{k})}{2\omega(\mathbf{k})}, R_3(\mathbf{k}) = \frac{\Delta \gamma_3(\mathbf{k})}{2\omega(\mathbf{k})}.$$

- ¹ P. W. Anderson, Mater. Res. Bull. **8**, 153 (1973); P. Fazekas and P. W. Anderson, Philos. Mag. **30**, 423 (1974).
² D. A. Huse and V. Elser, Phys. Rev. Lett. **60**, 2531 (1988).
³ Th. Jolicoeur and J. C. Le Guillou, Phys. Rev. B **40**, 2727 (1989).
⁴ B. Bernu, C. Lhuillier, and L. Pierre, Phys. Rev. Lett. **69**, 2590 (1992); B. Bernu, P. Lecheminant, C. Lhuillier, and L. Pierre, Phys. Rev. B **50**, 10048 (1994).
⁵ L. Capriotti, A. E. Trumper, and S. Sorella, Phys. Rev. Lett. **82**, 3899 (1999).
⁶ S. Sachdev, Phys. Rev. B **45**, 12377 (1992).
⁷ See a review in G. Misguich and C. Lhuillier, *Frustrated Spin Systems*, edited by H. T. Diep, (World-Scientific, Singapore, 2004).
⁸ A. B. Harris, C. Kallin, and A. J. Berlinsky, Phys. Rev. B **45**, 2899 (1992).
⁹ C. Zeng and V. Elser, Phys. Rev. B **42**, 8436 (1990).
¹⁰ J. T. Chalker and J. F. G. Eastmond, Phys. Rev. B **46**, 14201 (1992).
¹¹ C. Waldtmann, H. -U. Everts, B. Bernu, C. Lhuillier, P. Sindzingre, P. Lecheminant, L. Pierre, Eur. Phys. J. B **2**, 501 (1998).
¹² A. V. Syromyatnikov and S. V. Maleyev, Phys. Rev. B **66**, 132408 (2002); P. Nikolic and T. Senthil, Phys. Rev. B **68**, 214415 (2003).
¹³ C. Broholm, G. Aeppli, G. P. Espinosa, and A. S. Cooper, Phys. Rev. Lett. **65**, 3173 (1990); A. Keren *et al.*, Phys. Rev. B **53**, 6451 (1996); A. Fukaya *et al.*, Phys. Rev. Lett. **91**, 207603 (2003).
¹⁴ A. P. Ramirez, G. P. Espinosa, and A. S. Cooper, Phys. Rev. Lett. **64**, 2070 (1990); B. Martinez *et al.*, Phys. Rev. B **46**, 10786 (1992).
¹⁵ A. P. Ramirez, B. Hessen, and M. Winklemann, Phys. Rev. Lett. **84**, 2957 (2000).
¹⁶ P. Sindzingre, G. Misguich, C. Lhuillier, B. Bernu, L. Pierre, C. Waldtmann, and H. -U. Everts, Phys. Rev. Lett. **84**, 2953 (2000).
¹⁷ R. Budnik and Assa Auerbach, Phys. Rev. Lett. **93**, 187205 (2004).
¹⁸ Y. Ran, M. Hermele, P. A. Lee, and X. G. Wen, cond-mat/061141.
¹⁹ P. W. Anderson, Science **235**, 1196 (1987).
²⁰ D. P. Arovos and A. Auerbach, Phys. Rev. B **38**, 316 (1988); A. Auerbach and D. P. Arovos, Phys. Rev. Lett. **61**, 617 (1988).
²¹ A. Auerbach, *Interacting Electrons and Quantum Magnetism*, (Springer-Verlag, NY, 1994).
²² C. J. Gazza and H. A. Ceccatto, J. Phys.: Condens. Matter **5**, L135 (1993); L. O. Manuel, A. E. Trumper, and H. A. Ceccatto, Phys. Rev. B **57**, 8348 (1998).
²³ S. -Q. Shen and F. C. Zhang, Phys. Rev. B **66**, 172407 (2002).
²⁴ L. O. Manuel, A. E. Trumper, C. J. Gazza, and H. A. Ceccatto, Phys. Rev. B **50**, 1313 (1994).
²⁵ F. Wang and A. Vishwanath, Phys. Rev. B **74**, 174423 (2006).
²⁶ N. Read and D. M. Newns, J. Phys. C **16**, 3273 (1983).
²⁷ Y. J. Uemura, A. Keren, K. Kojima, L. P. Le, G. M. Luke, W. D. Wu, Y. Ajiro, T. Asano, Y. Kuriyama, M. Mekata, H. Kikuchi, and K. Kakurai, Phys. Rev. Lett. **73**, 3306 (1994).
²⁸ P. W. Anderson, *Concepts in Solids*, (World Scientific, Singapore, 1997).